Publication Year	2022
Acceptance in OA	2025-03-07T15:55:10Z
Title	MAORY/MORFEO at ELT: Thermal Control System preliminary design
Authors	ALIVERTI, Matteo, PARIANI, Giorgio, MAGRIN, DEMETRIO, REDAELLI, Edoardo Maria Alberto, DONISELLI, Simone, COLAPIETRO, Mirko, SALASNICH, Bernardo, DE CAPRIO, VINCENZO, CIANNIELLO, Vincenzo, EREDIA, Christian, CASCONE, Enrico, RIVA, Marco, CILIEGI, Paolo, DI GIAMMATTEO, Ugo
Publisher's version (DOI)	10.1117/12.2629908
Handle	http://hdl.handle.net/20.500.12386/36533
Serie	PROCEEDINGS OF SPIE
Volume	12185

MAORY/MORFEO@ELT: Thermal Control System preliminary design

Matteo Aliverti*[a], Giorgio Pariani[a], Demetrio Magrin[b], Edoardo Maria Alberto Redaelli[a], Simone Doniselli[a], Mirko Colapietro[a], Bernardo Salasnich[b], Vincenzo De Caprio[c], Vincenzo Cianniello[c], Christian Eredia[c], Enrico Cascone[c], Marco Riva[a], Paolo Ciliegi[d], Ugo di Giammatteo[d]

[a]INAF Osservatorio Astronomico di Brera, Via Emilio Bianchi 46, I 23807, Merate (LC), IT;
[b]INAF Osservatorio Astronomico di Padova, Vicolo dell'Osservatorio 5, 35122 Padova, IT;
[c]INAF Osservatorio Astronomico di Capodimonte, Salita Moiariello 16, I 81100 Napoli, IT;
[d]INAF Osservatorio di Astrofisica e Scienza dello Spazio di Bologna, Via Gobetti 93/3, Bologna, IT;

ABSTRACT

MORFEO (formerly known as MAORY) is an adaptive optics module able to compensate the wavefront disturbances affective the scientific observation. It will be installed on the straight-through port of the telescope Nasmyth platform to serve the first-light instrument MICADO and with the provision for a future second instrument. The module underwent the Preliminary Design Review in 2021 and is expected to be commissioned in 2029.

In this paper we present the current status of the Thermal Control System (ThCS) including the modifications required during the Preliminary Design Review. Due to the peculiar optical and mechanical design, a number of FEM and CFD analysis have been performed to verify the compliance of the system to the technical budget. The results of those analysis are then showed together with the current thermal and cooling circuits design derived from them.

1. INTRODUCTION

MORFEO is a post-focal module to be installed on the ELT Nasmyth platform A with two adaptive optics modes: SCAO and MCAO. A general overview of the instrument can be found in [1] while the optical design with its nominal optical performances, the tolerance analysis, and the stability analysis is presented in [2]. The mechanical design of the structure and the optomechanical elements are presented in [3] and [4] respectively while the instrument control hardware is the topic of [5]. The thermal behaviour of a large AO relay instrument with al long optical path such as MORFEO for the ELT has not been extensively studied in the past. For this reason, a large set of analyses have been performed and partially presented in the paper [6].

This proceeding is subsequent to said analysis as, once the overall philosophy has been defined, more detailed analyses have been performed and the design of the Thermal Control System (ThCS) has been developed towards the PDR.

It composed by five parts: in section 2 a brief overview of the design proposed for the MORFEO ThCS is presented including both the circuit design and the insulation panels design. Later the three main analyses performed are described: a brief discussion of the sensitivity analyses in section 3, fluid dynamics analyses in section 4 and thermoelastic analyses in section 5.

2. THCS DESIGN

The thermal design based on the analyses reported later, consists of a thermal enclosure surrounding the whole instrument (see Figure 1) and a series of cooling circuits used to maintain an adequate temperature in all the parts.

*matteo.aliverti@inaf.it; phone +39 347 1504637; http://www.brera.inaf.it/

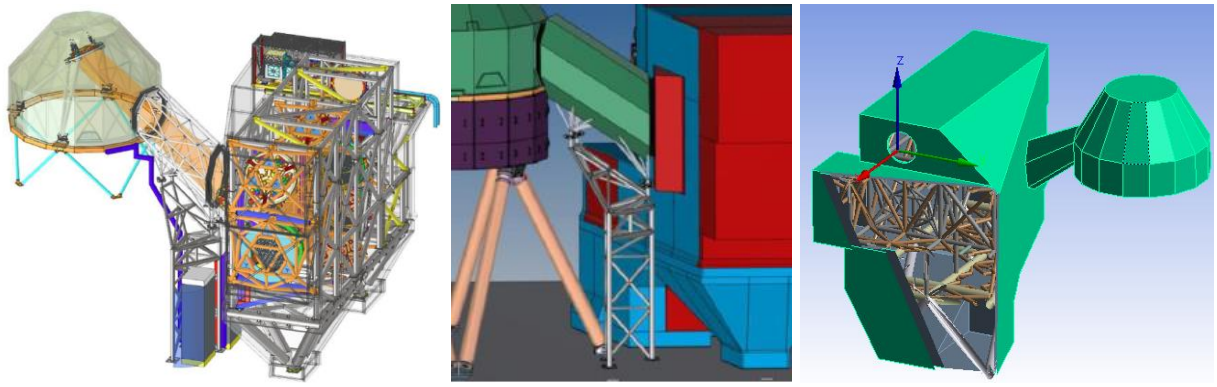

Figure 1. Overall view of MORFEO. Left: Mechanical design of the structure. Centre: view of the enclosure (red, blue and green). Right: simplified model used for the final thermoelastic analysis.

The design of the two parts is described hereafter.

2.1. Circuit design of the ThCS

At the ELT, MORFEO will have one SCP where the cooling fluid is provided, with a maximum flow of 30l/min. This flow is used to cool down two different circuits: one controls the temperature of all the elements located on the Nasmyth platform (see Figure 3) while the other controls the temperature of all the cabinets located on the intermediate platform (see Figure 2).

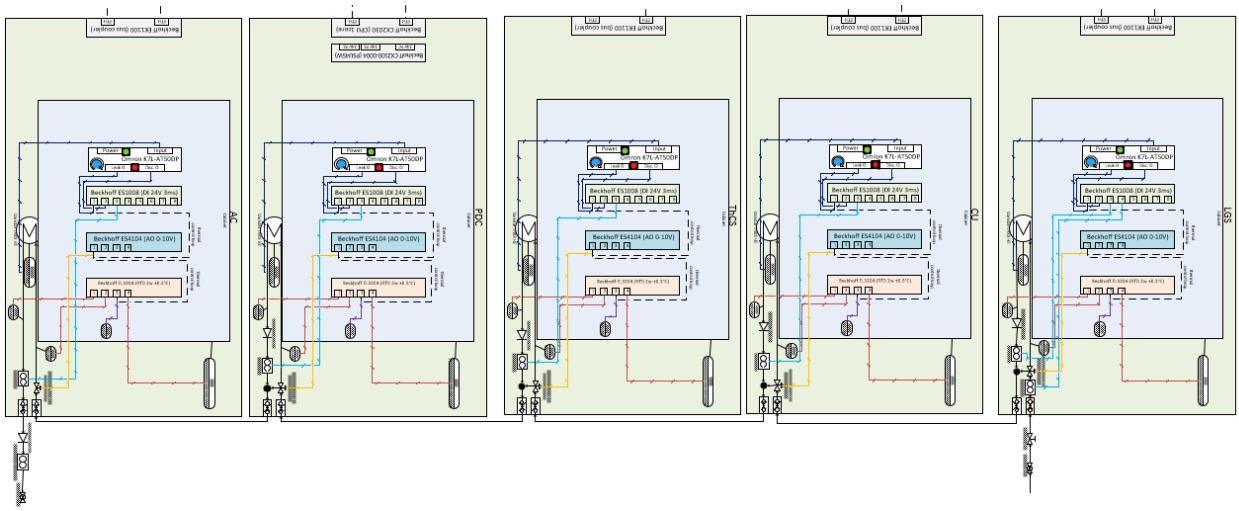

Figure 2. Overall view of the cooling system for the cabinets located on the intermediate platform.

In the intermediate platform the flows control the temperature of five thermally insulated cabinets in series to reduce the cooling flow. Each of those cabinets has a heat exchanger, a three-way valve, a check valve, a number of temperature sensors, a leak detector, and a flowmeter. All of them are identical with the exception of the first cabinet which has an extra flowmeter to check for the input flow and the last cabinet which has a 2-way valve instead of a 3-way vale to avoid short-circuits. This configuration allows for a safe thermal control of all the elements and to maintain a similar temperature between the outer skin of the cabinets and the environmental temperature.

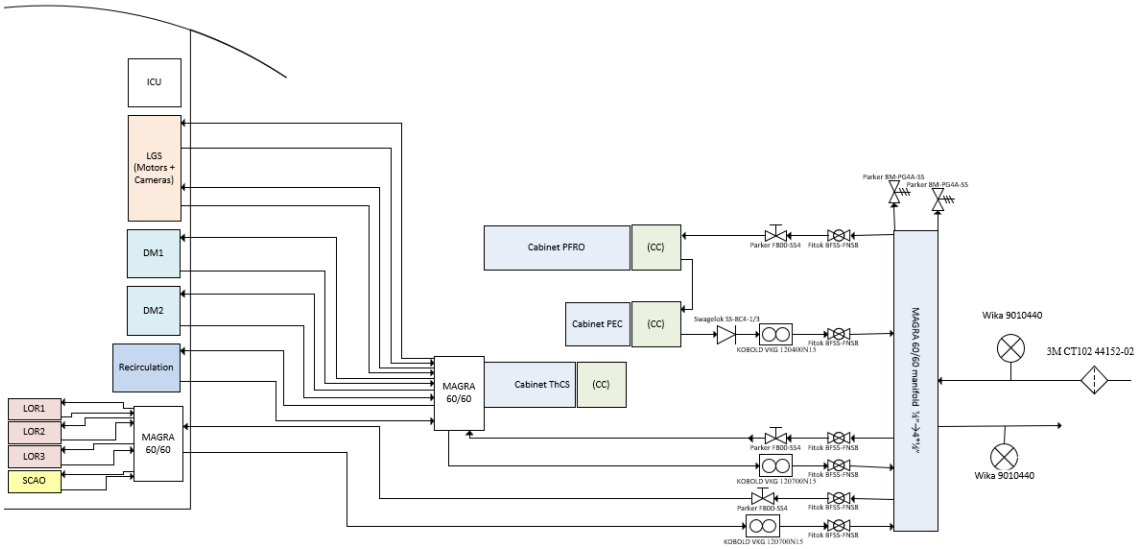

Figure 3. Overall schematic view of the MORFEO cooling distribution for the elements located on the Nasmyth platform.

The cooling on the Nasmyth platform works as follow: the fluid is split in 3 circuits via a passive manifold. The first cools two electronic cabinets in series, the second goes to an active manifold feeding the LGS, the DMs, and the recirculation system while the third goes to an active manifold feeding the three LOR modules and the SCAO.

The passive manifold includes flow indicators, manual valves, shut-off valves, purge valves, pressure gauges and a filter.

The active manifolds are shown in Figure 4 and Figure 5. They are composed by a 'passive' part (with manual valves, flow indicators, shut-off valves, purge valves, and check valves) and an active part (with Siemens VVP47 regulation valves, Bürkert normally closed valves, and IFM flowmeters).

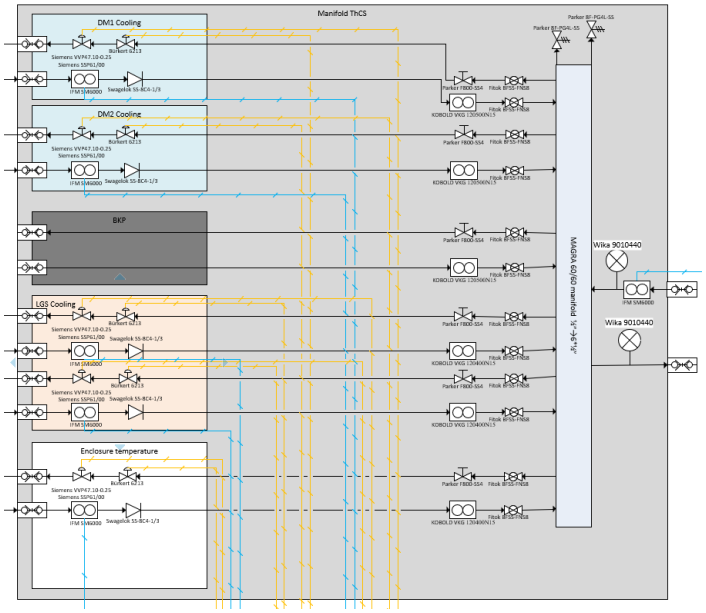

Figure 4. Schematic view of the active manifold used to recirculate the fluid to DMs, LGS, and Recirculation system.

The active part takes the information from the temperature, leakage, and humidity sensors located on the subsystem and regulates the flow towards the various components in order to have their temperature:

1. close to the temperature of the air inside the enclosure in the night-time
2. at the temperature expected at the beginning of next night in the daytime

An example of the interaction between the sensors and the valves is shown in Figure 6.

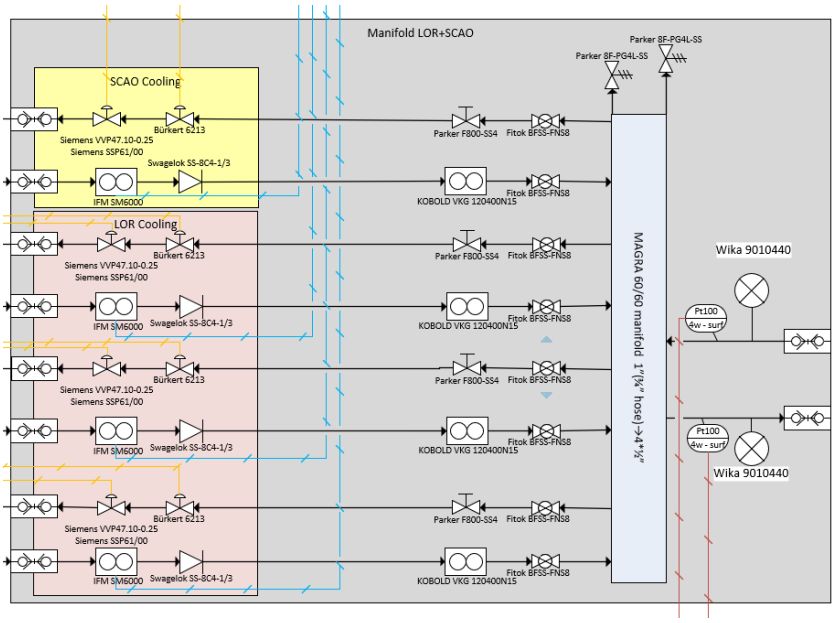

Figure 5. Schematic view of the active manifold used to recirculate the fluid to LOR and SCAO.

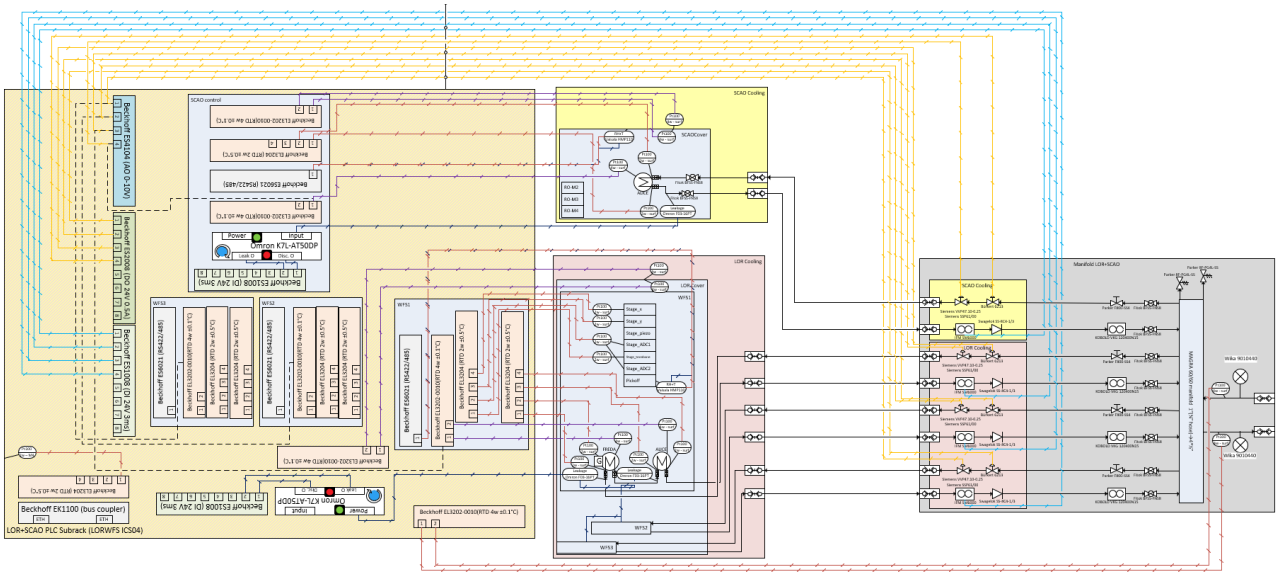

Figure 6. Schematic view of the thermal control system of the SCAO (yellow) and LOR (red). In orange the electronic modules located in the cabinet and in gray the manifold mounted on the side of the cabinet.

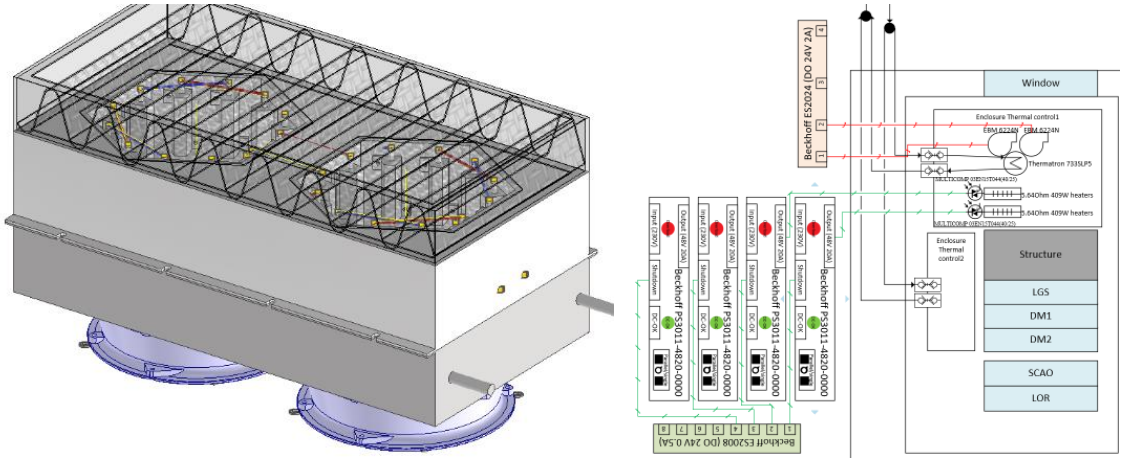

Figure 7. Left: recirculation module. Right: schematic view of the recirculation module.

In order to prepare the instrument for the next night, in addition to the change the temperature of the various components, a recirculation system has been foreseen (see Figure 7). It consists of two identical modules composed by two fans, a heat exchanger fed by the cooling circuit, 24 resistors coupled with thermostat switches, and an air filter.

This system shall be used to have a more homogenous temperature inside the instrument and to change the temperature of the whole MORFEO instrument (optomechanical elements, structure, and enclosure) in the daytime.

2.2. Enclosure design and analyses workflow

The enclosure, visible in Figure 1, is made out of multilayer panels thermally and mechanically connected to the MORFEO structure. The panels are composed by an external PIR panel and an inner plate of aluminium 1100. The PIR thickness is 70 mm and the aluminium one is 1 mm for the panels around the MORFEO main structure. The cover of the tube between MORFEO and MICADO has thicknesses of 100mm/2mm while the cover above MICADO has thicknesses of 70mm/2mm.

3. SENSITIVITY ANALYSES AND ANALYSES WORKFLOW

To identify the major players of the thermal induced effects in MORFEO, different analyses have been performed. Those included air temperature variations/gradients, air pressure variations, temperature difference/gradients between air and optical elements (the so-called “skin effect”), temperature difference between air and optical elements, uniform temperature variations of the Nasmyth, and temperature gradients of the structure in the various directions. A short summary of them has already been presented in [6] together with a 3-day long time-varying thermoelastic analysis with a first enclosure developed following the results of said analyses.

Once the baseline has been defined a more refined enclosure designed has been developed (see section 2.2) and 3D CFD sensitivity analyses have been done to evaluate the “skin effect” together with 3-day long time-varying thermoelastic analysis both in the median conditions and the operational conditions. All the other analyses have been also updated in parallel but thy will not be presented here.

Said conditions consider an external temperature following the profiles shown in Figure 8. The median one has been obtained combining the expected variations on the site provided by ESO while the operational one has been obtained stretching the previous intra-day variation until the operational gradients (part of the ESO requirements) are met and applying the inter-day variations requested in the “operational conditions” requirements by ESO.

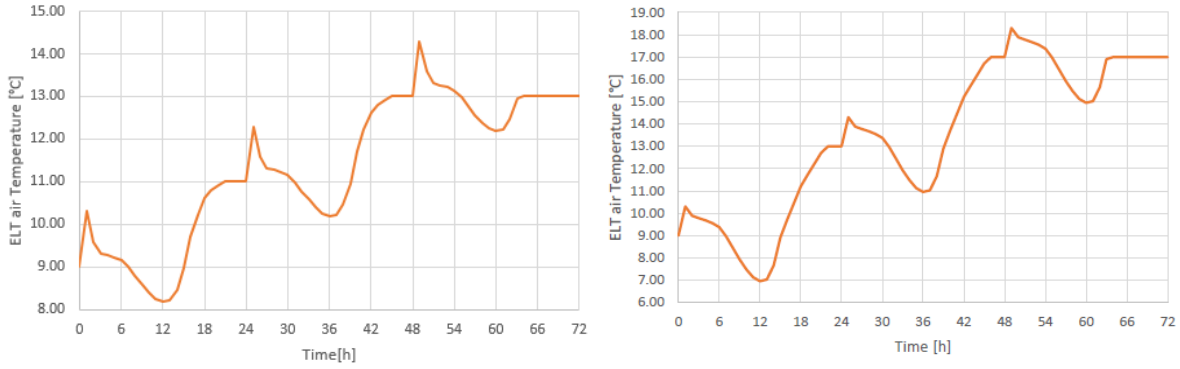

Figure 8. Temperature profile used for the time-dependant analyses Left: median conditions. Right: operational conditions.

4. TEMPERATURE DIFFERENCE BETWEEN AIR AND (OPTICAL) ELEMENTS – 3D ANALYSIS

To better describe the effect on the optical system of the temperature difference between air and optical elements and, therefore, to define if it is a critical aspect, 3D CFD simulations have been performed on each optical element, considering a uniform temperature difference between the element and the air of ±1°C (reasonable value considering the time-varying analyses performed).

Each optical element has been modelled and two examples are shown in Figure 9.

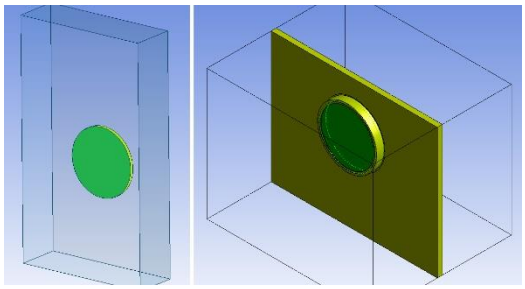

Figure 9. Geometry of the 3D models. Right: model for the plate; in green the optical element, in yellow the PIR insulation and the Viton and steel elements. Left: model for all the other optical elements; in green the walls with imposed temperature

The plate (right) has been modelled considering a portion of inner air sized as the MORFEO structure, and a portion of outer air. An intermediate surface made of PIR, Viton, and steel has been modelled to simulate the cover and its interface with the optical element. Regarding the boundary conditions, in the inner part the top and lateral walls have been fixed to the 'inner temperature' while the front and the bottom surface are inflow/outflow surfaces. The inner PIR surface has also been fixed at the 'inner temperature' to consider for the high thermal capacity of the structure. In the outer part, one lateral surface has an inflow of 1m/s while the other is an outflow. The front, top, and bottom surfaces are simulated as adiabatic walls for the sake of stability in the simulation. The 'outer temperature' has been kept at -2°C with respect to the 'inner temperature'.

The other optical elements (left) have been modelled imposing a wall temperature of ±1°C with respect to the air temperature on the three surfaces of the mirror (front, back, and side). Regarding the boundary conditions, all the surfaces are inflow or outflow depending on the expected direction of the air. The expected flow speed is between 0.15 and 0.21m/s.

A finer mesh around the optical elements to cover the moving air layer (between 10 and 15 mm depending on the element) has been applied. Note that all the elements have been simulated independently and, therefore, there is no cross talk between them. Moreover, the effect of the walls, except for the plate case, has not been considered.

An example of the results obtained for a strongly tilted mirror (M7) is shown in Figure 10. This element is facing upward and, when its temperature is above the surrounding air one, we have columns formation that create high spatial frequency

disturbances. When its temperature is lower, instead, the flow has no columns and the results are similar to the ones obtained in the 2D simulations shown in [6]. The opposite conditions are observed for the mirrors facing downwards.

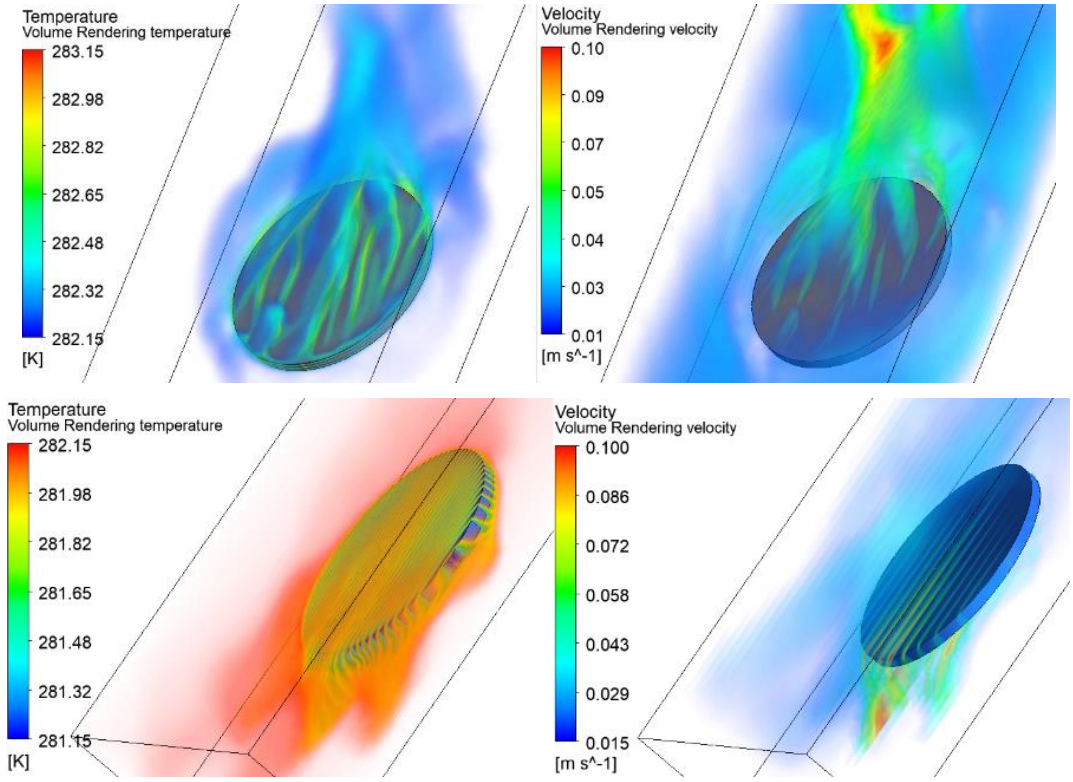

Figure 10. M7 results when the mirror is hotter (above) or colder (below) than the surrounding air. On the left the temperature profile and on the right the velocity profile.

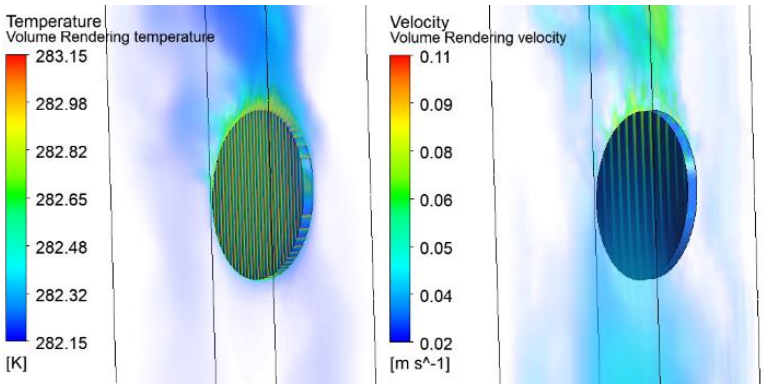

Figure 11. M11 results when the mirror is hotter than the surrounding air. On the left the temperature profile and on the right the velocity profile.

When the mirror is almost vertical (e.g., M11 in Figure 11) there are no columns and, again, the results are similar to the ones obtained in the 2D simulations shown in [6].

These results have been evaluated exporting the air temperature from a number of layers in front of and perpendicular to the mirrors and integrating the corresponding optical path difference values along the element normal. To be conservative, the refractive index has been calculated at 589 nm (LGS) in any point of the space facing the optical element.

An example of the results is shown in Figure 12.

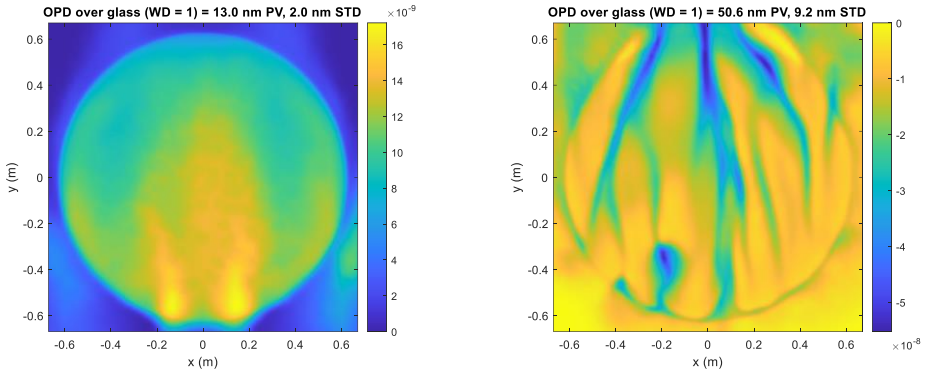

Figure 12. OPD in front of M7, considering a wedge factor of 1, for a negative (left) and positive (right) temperature variation between the element and the air. The values refer to the whole glass surface.

Since the temperature of each element is not knows a priori, the worst OPD between the two cases has been considered, and the corresponding surface has been inserted into the nominal Zemax model, using the grid sag surface type.

The results of the simulation without any compensation are reported in Figure 13 and Figure 14. No remarkable changes have been observed on the pointing, pupil and metapupil quality, and footprints on the optics. The WFE is very close to the nominal condition for both the technical and MICADO FoVs. The arithmetic difference with respect to the nominal design is reported in Figure 14, where a maximum WFE of 16 nm RMS has been observed all over the technical FoV.

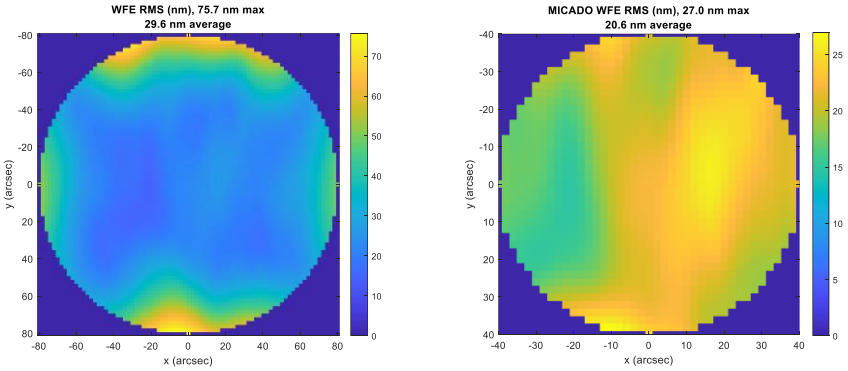

Figure 13. RMS WFE maps for the technical FoV (left) and MICADO FoV (right) due to the air skin effect in front of the optics.

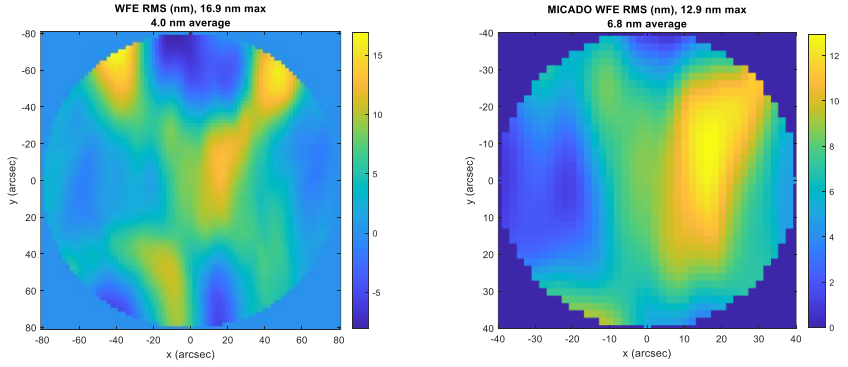

Figure 14. Differential RMS WFE maps for the technical FoV (left) and MICADO FoV (right) as respect to the nominal design.

The major effects of the air refractive index variation in front of the elements are linked to the distortion. The residuals are larger than in the nominal design, where residuals are negligible after the 5th order correction, due to the presence of high

order variations of the distortion pattern. High orders are present also in the intra-epoch distortion variation, but the values are in line with the nominal design, and well below the requirement.

Since the major players for the distortion are the elements placed in proximity of the focal planes, the plate is most probably the responsible of the high order distortion residuals. Moreover, the external surface of the plate is the most affected by air disturbances. A strategy to mitigate this effect in proximity of the plate, e.g., baffles or isolations between the pre-focal station and the plate, will be considered in the next phase of the project. The main unknown in the astrometric precision, which is also quite difficult to be simulated, is the temporal variability of this effect, which affects the validity of the distortion calibrations.

5. THERMOELASTIC ANALYSES

The results presented in the previous sections together have been used to define the design of the whole enclosure while the thermoelastic time-depended analyses have been used to fine tune it. The design imported in the simulation software is shown on the right of Figure 1. The model is composed by the steel structure (beam elements), the external PIR panels (solid elements), the inner aluminium layer (shell elements) and a concentrated thermal point to simulate the structure holding the panels above MICADO. This model has been used to simulate the thermoelastic behaviour of MORFEO in a median condition (profile in Figure 8, left) and an operational condition (profile in Figure 8, right).

The structure has been kinematically connected to the Nasmyth through its 3 legs to remove the effect of the Nasmyth deformations. Those deformations will be taken into consideration as soon as more data on the Nasmyth platform behaviour is available.

A conservative convection coefficient of 10W/m^{2}K has been applied over the entire outer layer together with a radiative contribution (low emissivity paint with a coefficient of 0.1725). A surface-to-surface radiation between the aluminium panels has also been considered (IR black paint with a coefficient of 0.9).

5.1. Median night performances – Thermoelastic analysis

The temperature distribution at the end of the first and the second night on the aluminium part of the enclosure and on the structure is shown in Figure 15 and Figure 16. The maximum deviations on the cover are located on the tube between MORFEO and MICADO while on the structure it is located at its core, near the M9 mirror.

The average temperature of the aluminium panels over the 3 days are shown in Figure 17, while the average temperature of the components around the MORFEO structure are shown in Figure 18. The obtained results are compatible with the ones obtained in the simplified analyses shown in [6]. As the average temperatures of the components inside MORFEO remain close to each other, the behaviour with the recirculation system activated can be expected to be similar to the one shown there.

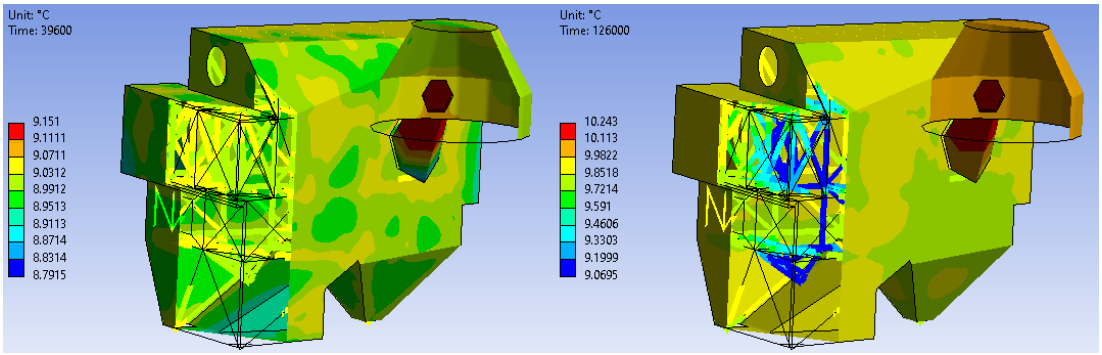

Figure 15. Temperature of the structure and the aluminium part of the enclosure after 11 hours (left) and after 35 hours (right).

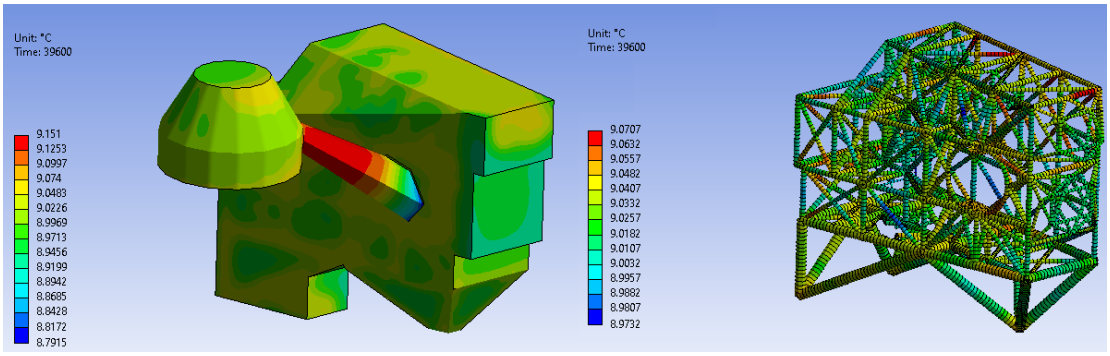

Figure 16. Temperature after 11 hours. On the left the aluminium part of the enclosure and on the right the steel structure.

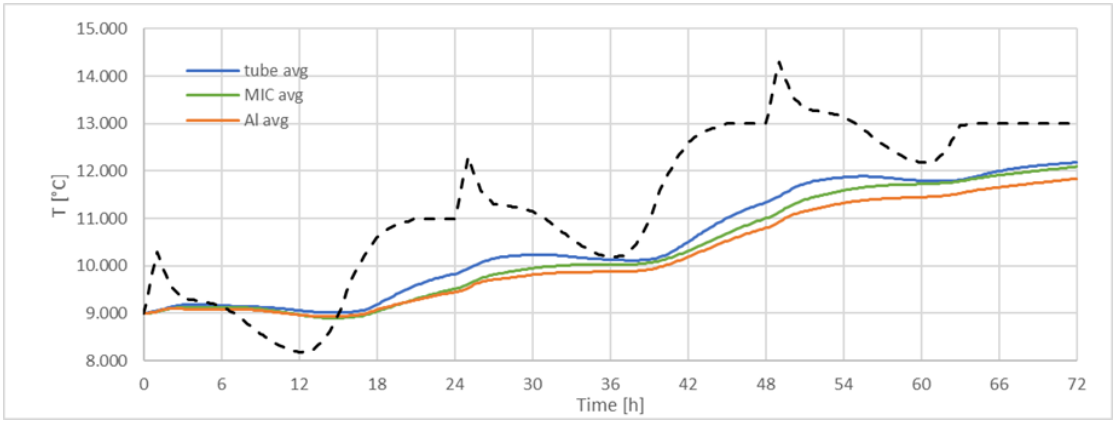

Figure 17. Temperature profile along 3 days. Average temperature of the aluminium surface around MORFEO, the tube and the hat above MICADO.

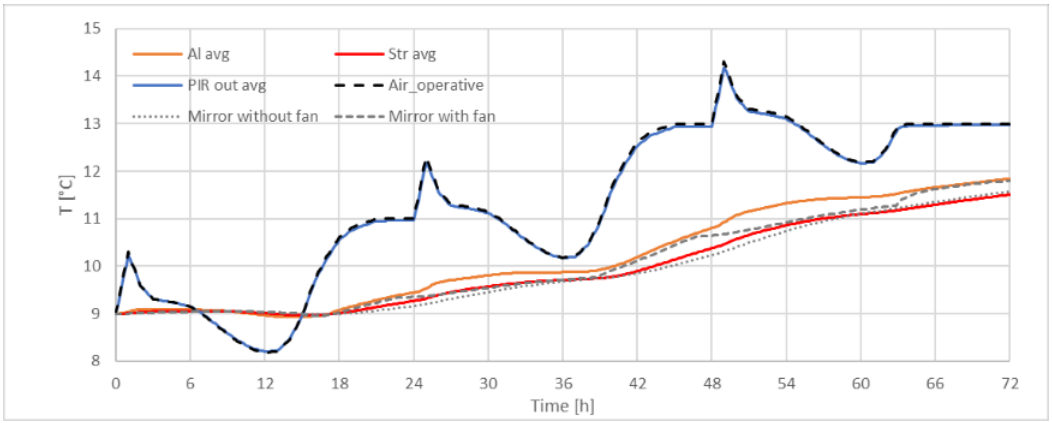

Figure 18. Temperature profile along 3 days. Average temperature of the element around the MORFEO structure (structure, aluminium, outer PIR temperature and mirrors).

The deformations on the steel structure have been finally calculated applying the temperature distributions in a static structural analysis, and the obtained deformations imported in the Zemax model as displacements and rotations of the I/F points with the opto-mechanical assemblies. M12 has been considered fixed over MICADO. The deformations at the end of the first and second nights are shown in Figure 19. Two examples of the movements applied to M6 and M7 are reported in Figure 20.

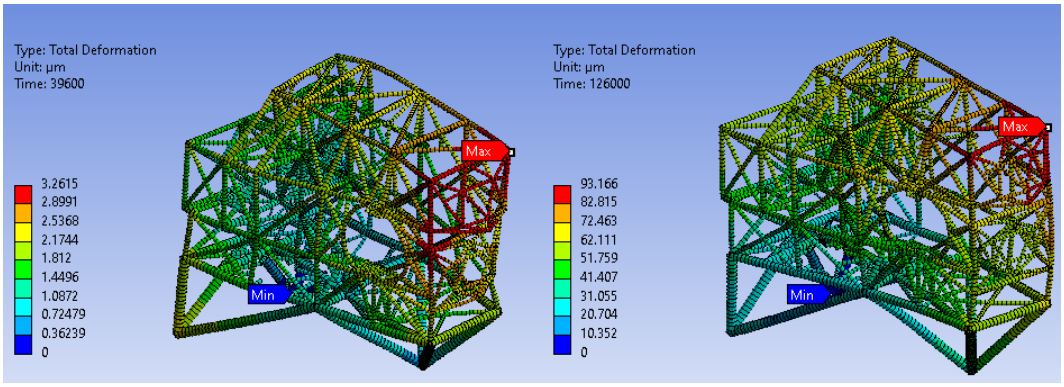

Figure 19. Total deformations of the structure after 11 hours (left) and after 35 hours (right).

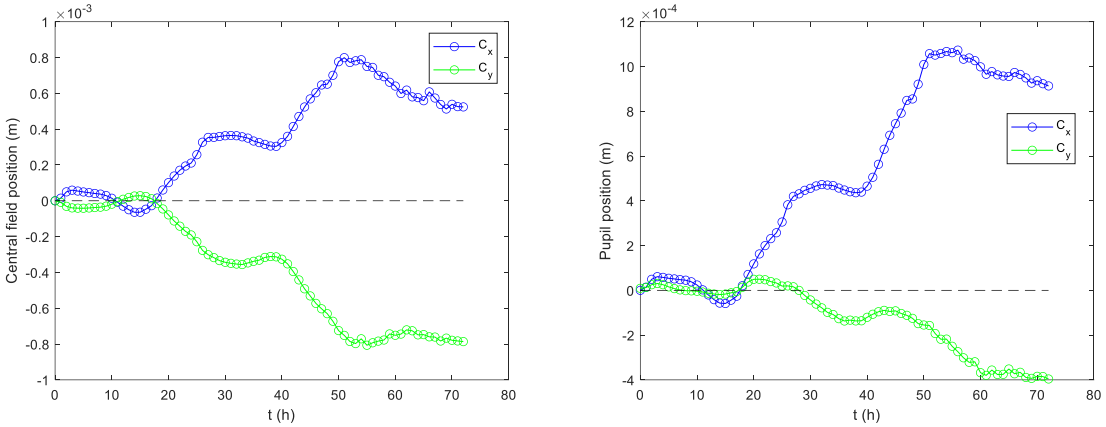

Figure 20. Central field position on the MORFEO exit focal plane (left) and exit pupil position as function of time considering the median temperature profile.

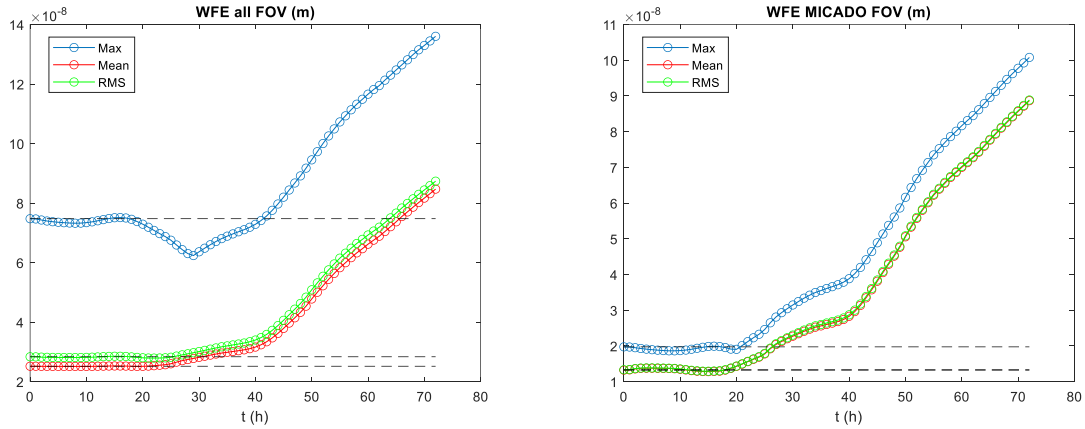

Figure 21. WFE on the full FOV (left) and MICADO FOV (right) as function of time considering the median temperature profile.

The effects of the thermo-elastic deformations as function of time on WFE, central field centroid position (pointing), exit pupil displacement, and inter-epoch distortion variation have been then computed and shown in Figure 20, Figure 21, and Figure 22.

The main effects after the three days are pointing (a mm on the exit focal plane), exit pupil displacement (a mm) and WFE (degradation up to a maximum of 100 nm RMS on the MICADO FoV, due mainly to focus and astigmatism). The inter-epoch distortion variation performance is completely recovered after the 3rd order polynomial fitting.

In order to verify the capability of the system to recover the full performance, the "MORFEO collimation procedure" has been applied before each night. In this case the degrees of freedom are M10 (with piston, tip/tilt), M12 (with tip/tilt), and the MICADO de-rotator (clock). The fields have been optimized on five reference stars at the edge of the MICADO FoV. The effect of the collimation procedure is clear in Figure 23, where the central field is moved to zero before each night. The WFE is also minimized before each night (Figure 24). The effect on the interepoch distortion variation is reported in Figure 25.

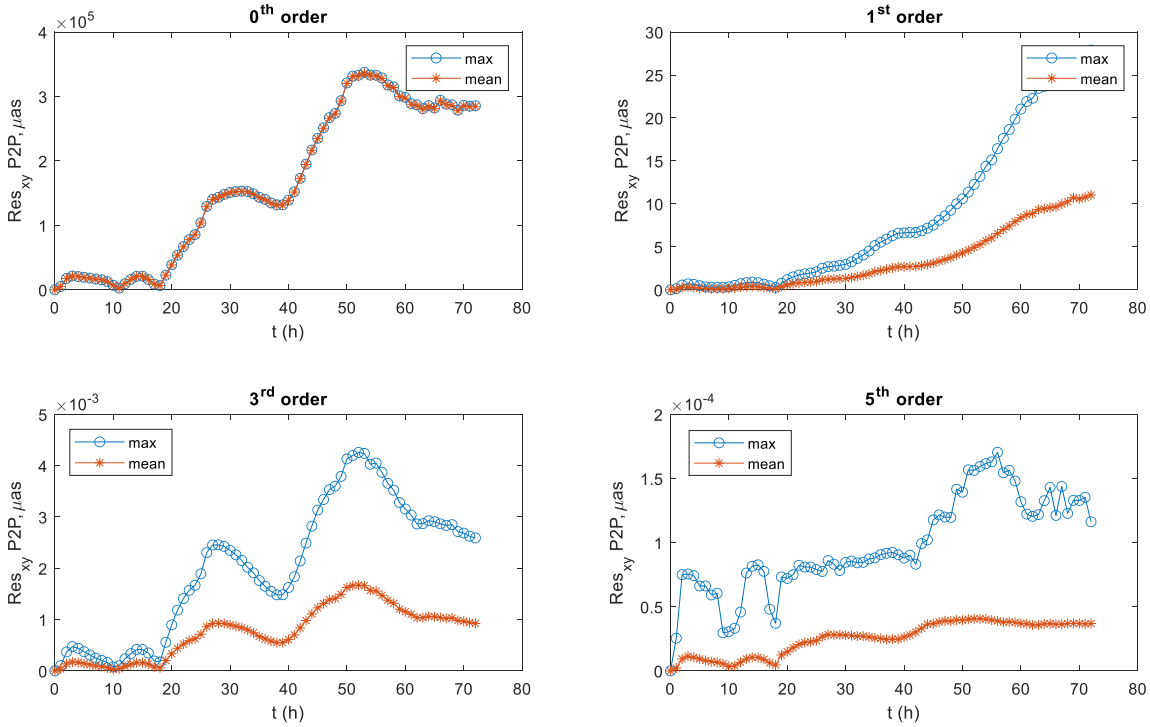

Figure 22: Inter-epoch distortion variation after polynomial fitting as function of time.

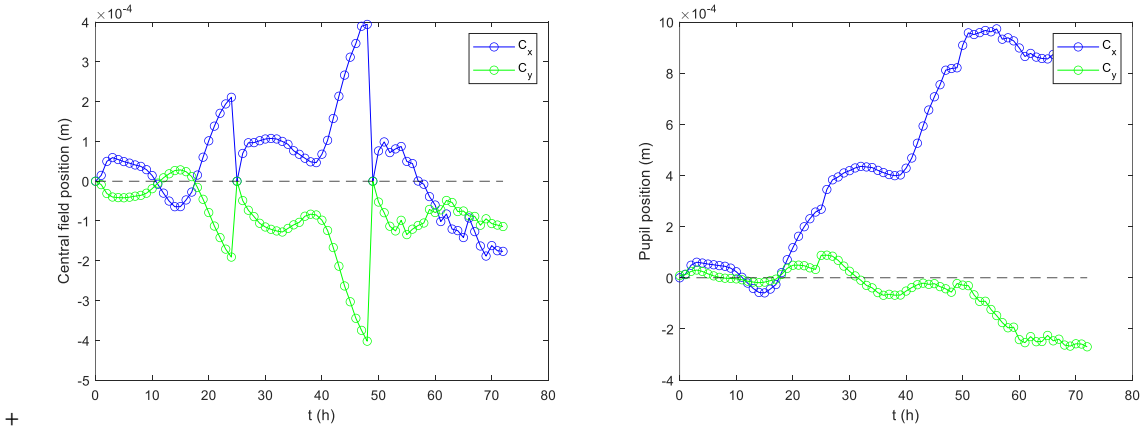

Figure 23. Central field position on the MORFEO exit focal plane (left) and exit pupil position as function of time.

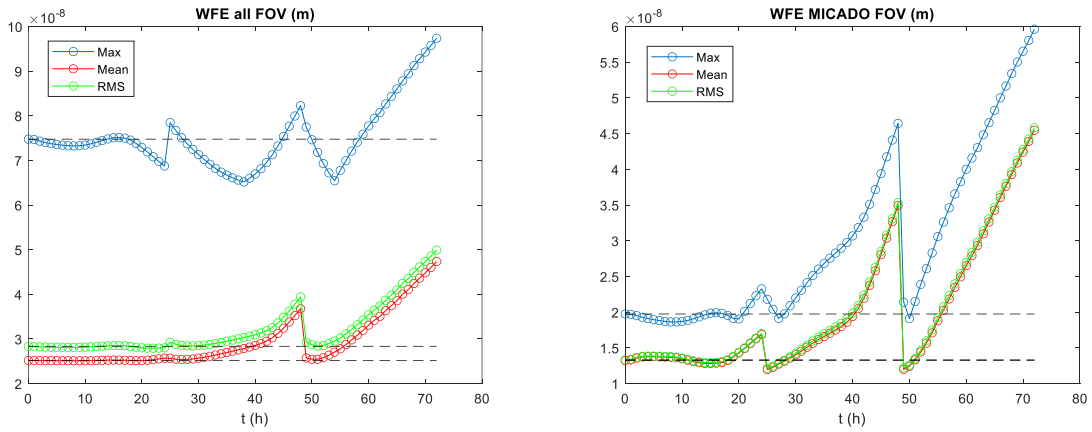

Figure 24. WFE on the full FOV (left) and MICADO FOV (right) as function of time.

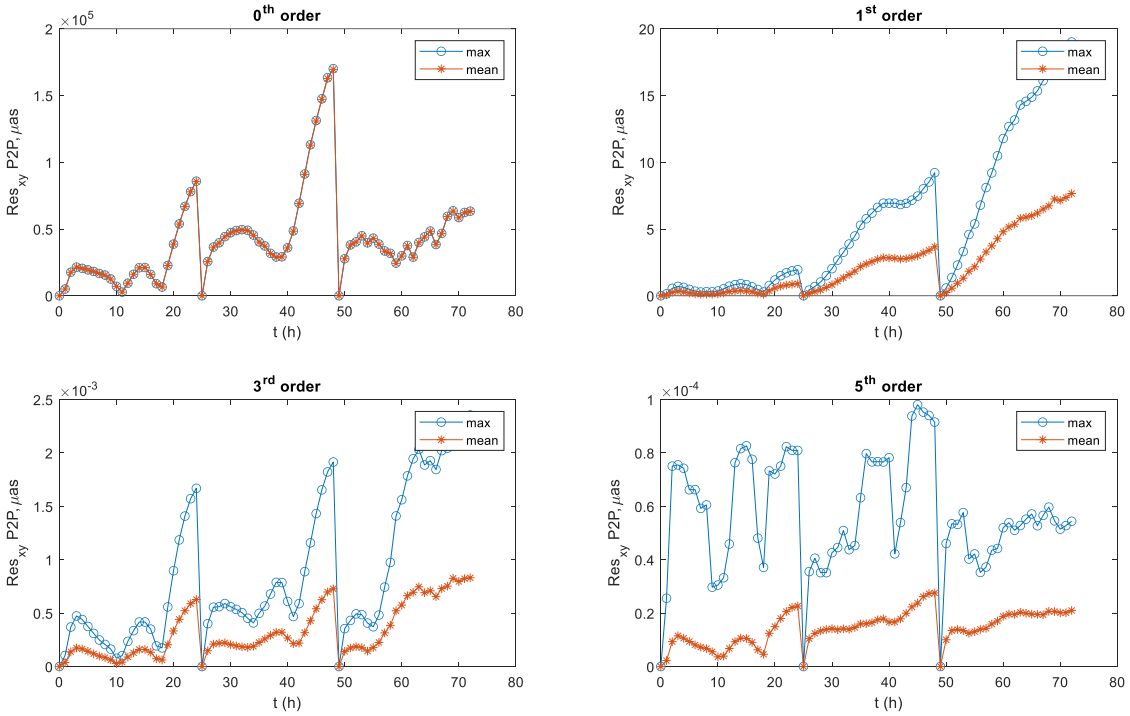

Figure 25: Inter-epoch distortion variation after polynomial fitting as function of time.

5.2. Median night performances – Temperature difference between air and optical element

Due to the low thermal conductivity of the optomechanical elements the preliminary evaluation of the mirrors' temperatures has been done as already presented in section 4. The temperature distribution of the aluminium part of the envelope around MORFEO and of the structure are summarized in Figure 26 for the first 48h.

In the first night, the temperature of the structure remains in between a ±0.1K band while the temperature of the panels is in a ±0.2K band. In the second night, the minimum temperature of the structure remains at 9°C while the maximum increase up to 10°C. The panels have a maximum temperature of about 10°C and a minimum temperature increasing from 9.3°C to 9.6°C during the night.

It is worth recalling that this model considers conduction and radiation between the panels, conduction in the structure and convection between optical elements and panels. The natural convection during the night and the forced convection during the day will reduce the amplitude of those variations.

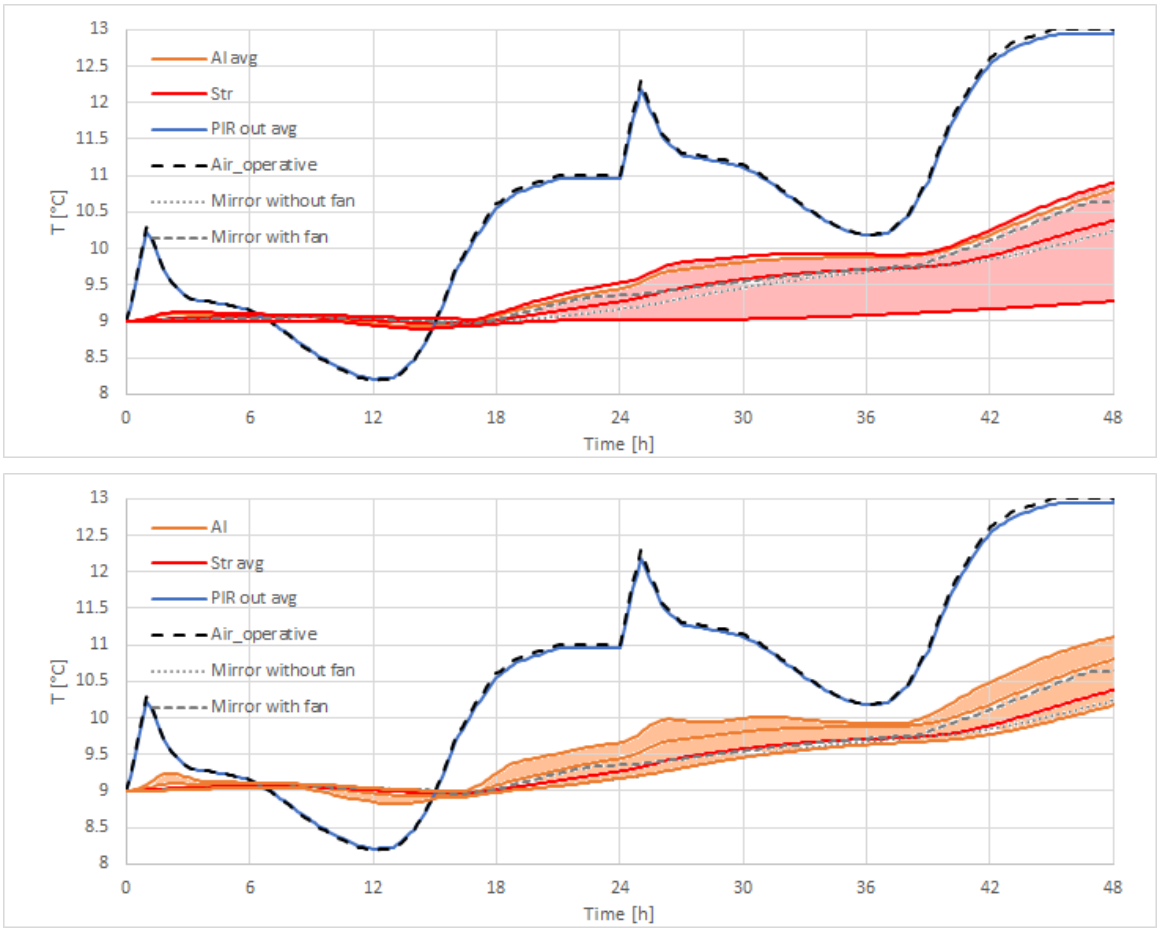

Figure 26. Temperature distribution of the structure (above) and the aluminium surface around MORFEO (below) in the 'median conditions' simulation. The 3 lines indicate the minimum, maximum, and average conditions. Only the first 48 hours are shown for clarity.

5.3. Operational night performances

The same analysis has been performed considering the 'operational conditions' (see Figure 8). The numerical results are not reported here but the same approach has been applied. In this case, in addition to the usual recalibration at the beginning of each night, a more frequent collimation (every 4 hours) during the 3rd day simulated.

6. CONCLUSIONS AND FUTURE DEVELOPMENTS

In this paper, the design of the MORFEO thermal control system developed for the Preliminary Design Review of the instrument has been presented.

Then, the results of the analyses dedicated to the baseline (passive cover thermally connected to the structure, as defined in [6]) have been shown. Those analyses have been used to refine the design of the thermal cover and to have a preliminary evaluation of the optical effects due to thermal disturbances.

The results obtained in section 5 proved that the difference between the optical elements and the air temperature used for the simulations presented in section 4 (1 K for the mirrors, 2 K for the plate) where a reasonable yet conservative assumption.

After the procedure involving pointing and collimation, no residuals remain on the WFE for the considered displacements.

Various other simulations are planned from the thermal point of view. They have not been evaluated yet due to time restrictions, because additional information is needed, and because the MORFEO design must be in a more advanced stage in order to have meaningful results.

Those include, in no particular order:

1. an evaluation of the Nasmyth effect in a time-dependant thermoelastic simulation (MORFEO deformation and MORFEO-MICADO displacement)
2. adding the LGS objective structure in a time-dependant thermoelastic simulation
3. adding the DMs, the LGS module in a time-dependant simulation to evaluate the cooling flow required and a subsequent CFD to evaluate the cooling flow effect on the optical quality
4. a complete CFD simulation of all the optical elements and the cover to be evaluated as non-sequential in Zemax
5. an improved CFD simulation of the entrance plate
6. a CFD simulation for the optomechanical motors
7. a FEM+CFD simulation of the M12→SCAO→LOR→MICADO elements to reduce the optical disturbances and to tune the LOR's cooling.

REFERENCES

[1] CILIEGI, Paolo, et al. MAORY/MORFEO@ELT: general overview up to the preliminary design and a look towards the final design. In: *Adaptive Optics Systems VIII*. SPIE, 2022.

[2] PARIANI, Giorgio, et al. MORFEO optical design and performances: status at preliminary design review. In: *Adaptive Optics Systems VIII*. SPIE, 2022.

[3] DE CAPRIO, Vincenzo, et al. Mechanical design overview for the Main Structure of MAORY/MORFEO. In: *Ground-based and Airborne Instrumentation for Astronomy IX*. SPIE, 2022.

[4] REDAELLI, Edoardo Maria Alberto, et al. MAORY@ELT: Optomechanical preliminary design. In: *Adaptive Optics Systems VIII*. SPIE, 2022.

[5] CASCONE, Enrico, et al. General overview of MORFEO (formerly known as MAORY) Instrument Control Hardware design. In: *Ground-based and Airborne Instrumentation for Astronomy IX*. SPIE, 2022.

[6] ALIVERTI, Matteo, et al. MAORY thermal behaviour. In: Modeling, Systems Engineering, and Project Management for Astronomy IX. SPIE, 2020. p. 367-382.